

**Flexible Conductive Composite Integrated with Personal Earphone
for Wireless, Real-time Monitoring of Electrophysiological Signs**Joong Hoon Lee, Ji-Young Hwang, Jia Zhu, Ha Ryeon Hwang, Seung
Min Lee, Huanyu Cheng, Sang-Hoon Lee, and SukWon HwangACS Appl. Mater. Interfaces, **Just Accepted Manuscript** • DOI: 10.1021/acsami.8b06484 • Publication Date (Web): 05 Jun 2018Downloaded from <http://pubs.acs.org> on June 5, 2018**Just Accepted**

"Just Accepted" manuscripts have been peer-reviewed and accepted for publication. They are posted online prior to technical editing, formatting for publication and author proofing. The American Chemical Society provides "Just Accepted" as a service to the research community to expedite the dissemination of scientific material as soon as possible after acceptance. "Just Accepted" manuscripts appear in full in PDF format accompanied by an HTML abstract. "Just Accepted" manuscripts have been fully peer reviewed, but should not be considered the official version of record. They are citable by the Digital Object Identifier (DOI®). "Just Accepted" is an optional service offered to authors. Therefore, the "Just Accepted" Web site may not include all articles that will be published in the journal. After a manuscript is technically edited and formatted, it will be removed from the "Just Accepted" Web site and published as an ASAP article. Note that technical editing may introduce minor changes to the manuscript text and/or graphics which could affect content, and all legal disclaimers and ethical guidelines that apply to the journal pertain. ACS cannot be held responsible for errors or consequences arising from the use of information contained in these "Just Accepted" manuscripts.



1
2
3
4
5
6
7 Flexible Conductive Composite Integrated with
8
9
10
11 Personal Earphone for Wireless, Real-time
12
13
14
15 Monitoring of Electrophysiological Signs
16
17
18
19

20 *Joong Hoon Lee,^a Ji-Young Hwang,^b Jia Zhu,^c Ha Ryeon Hwang,^a Seung Min Lee,^e Huanyu*
21 *Cheng,^{c,d} Sang-Hoon Lee,^a and Suk-Won Hwang^{*,a}*
22
23
24
25

26 ^aKU-KIST Graduate School of Converging Science and Technology, Korea University, 145,
27
28 Anam-ro, Seongbuk-gu, Seoul, 02841, Republic of Korea
29
30

31 ^bKorea Institute of Carbon Convergence Technology, 110-11, Ballyong-ro, Deokjin-gu, Jeonju,
32
33 54853, Republic of Korea
34
35

36
37 ^cMaterials Research Institute, ^dDepartment of Engineering Science and Mechanics, The
38
39 Pennsylvania State University, University Park, Pennsylvania, 16802, USA
40
41

42
43 ^eSchool of Electrical Engineering, Kookmin University, 77, Jeongneung-ro, Seongbuk-gu, Seoul,
44
45 02707, Republic of Korea
46
47

48 KEYWORDS: elastomeric composites, flexible, wearable electronics, wireless, EEG recordings
49
50
51
52
53
54
55
56
57
58
59
60

ABSTRACT

We introduce optimized elastomeric conductive electrodes using a mixture of silver nanowires (AgNWs) with carbon nanotubes/polydimethylsiloxane (CNTs/PDMS), to build a portable earphone type of wearable system that is designed to enable recording electrophysiological activities as well as listening music at the same time. A custom-built, plastic frame integrated with soft, deformable fabric-based memory foam of earmuffs facilitates essential electronic components, such as conductive elastomers, metal strips, signal transducers and a speaker. Such platform incorporates with accessory cables to attain wireless, real-time monitoring of electrical potentials whose information can be displayed on a cell phone during outdoor activities and music appreciation. Careful evaluations on experimental results reveal that the performance of fabricated dry electrodes are comparable to that of commercial wet electrodes, and position-dependent signal behaviors provide a route toward accomplishing maximized signal quality. This research offers a facile approach for a wearable healthcare monitor via integration of soft electronic constituents with personal belongings.

INTRODUCTION

Electronic materials, devices and circuits with superior mechanical properties create a flexible, stretchable electronic systems capable of applying to various application areas that might not be effectively addressed by conventional, rigid types of electronics, such as skin-based electronic tattoos¹⁻⁴ and implantable electronic devices⁵⁻⁸ for healthcare monitoring and therapeutic treatments. Recent approaches to achieve such technologies focused on: 1) structural modifications using diverse shapes of geometrical configurations,⁹⁻¹¹ 2) employments of intact, synthetic and composite electronic materials¹²⁻¹⁴ that have capability of being pliable without noticeable changes in electrical performance, in response to externally applied mechanical deformations. The former approaches exploited inorganic-based materials with particular structures to achieve large-area, high performance, and scalable manufacturing procedures, while the latter cases have advantages of extensive application abilities with facile layouts and fabrication strategies, and low-cost process over the former cases, through intrinsically soft materials-based components suitable for integration with wearable electronic systems. Examples in the materials context include nano-scaled conductive materials with several formats, ranging from metallic nanowires,^{15,16} to carbon nanotubes,¹⁷⁻²² graphene,²³⁻²⁵ and polymers,²⁶ printed/dispersed onto/in elastomeric matrices. These elastomeric composites provide particular benefits over other conductive materials, such as enhancement of mechanically conformal contacts at interfaces between the skin and electrodes, leading to allowance of recording high quality of electrophysiological signals.²⁷⁻²⁹ Here, we report a customized earphone that can monitor electrophysiological (EP) signals in a wireless, real-time mode, in addition to concurrently perform its original listening function. The following describes studies of fundamental electrical/physical characteristics of elastic, disposable composite materials,

theoretical evaluations, system-level operating capability and its potential application in practical use.

RESULTS AND DISCUSSION

Figure 1 illustrates a typical canal-typed earphone as a simple, comfortable and user-friendly interface for both recording electrophysiological activities and listening to music. The personalized EEG earphone consists of two components: a 3D-printed plastic frame including shielded electrical wires with a speaker (Figure 1a); a conductive composite elastomer for electrodes combined with disposable memory form (Figure 1b). The plastic encasement in a usual earphone shape was fabricated via a 3D printer (LITHO, Illuminaid) using light cured resins, and designed to provide the function of music and data pathway to accommodate signals transport. Small speakers are placed inside the earphone frame for providing sound like a generic earphone. A conductive double-sided bonding tape (copper, thickness $\sim 100\ \mu\text{m}$) was laminated onto an extended region of the plastic frame, providing electrical connections to both the fabric tape of the soft ear cushion and signal transmission lines. The three sound lines (two source and one GND) and three signal lines (source, reference and GND) are shielded by elastic thermal contraction tubes. (See Video S1 for additional information).

A highly deformable and conductive composite elastomer of AgNWs/CNTs/PDMS provides mechanically conformal contact between ear canals and electrodes, leading to reliable, continuous recording of electrophysiological signals. The detailed information of fabrication methods of AgNWs/CNTs/PDMS is presented in Figure S1 and microstructures and layers appear in Figure 1b. Each side of the EEG earphone in Figure 1c serves as the reference and ground electrodes (left side), and source electrodes (right side), whose recorded information is

processed via wireless signal acquisition circuit (Figure 1d and S2a), and transferred to consumer electronics such as a smart phone and laptop (Figure 1e and Figure S2b-c).

Measured impedances of elastomeric conductive nanocomposite (AgNWs/CNTs/PDMS) in various mixing ratios of AgNWs and CNTs appear in Figure 2. Impedance changes as a function of frequency for different weight percent (wt %) of AgNWs at the fixed value of 5 wt % CNTs exhibited that the conductivity of elastomeric composites was improved with addition of appropriate amount of AgNWs to CNTs (Figure S3a). The optimized condition reveals a dramatic enhancement of electrical property, i.e. impedance decrease three and ten orders of magnitude, compared to those values of independent CNTs- and AgNWs-based elastomers (Figure 2a). Images of scanning electron microscope and schematic illustrations indicate the detailed microstructures of each composite, explaining improved electrical properties depending on the formation of constituent materials (Figure S3b). Figure 2b illustrates measurements of skin-electrode impedance of a composite, as benchmarked against a commercial, standard Ag/AgCl electrode. Such resulting conductivity is relatively improved than that of a previous result³⁰ and comparable to that of wet type electrodes (See Figure S4 for additional information).

Assessment of system crosstalk is necessary to record electrophysiological signals, e.g. EEG, as well as listen to music at the same time. Since EEG signals have different frequency bands from musical sounds, the EEG signals are not directly influenced by different level of the music sound.^{31,32} The resulting EEG power spectrum (black line) in Figure 2c exhibited no signs of undesired music interferences (red line) in EEG signal band during measurement while small musical interference only detected over 40 Hz. Nevertheless, unexpected noises can be further reduced by an analog band pass filter and post signal processing techniques, and the signals of interest can be enhanced with a high gain amplifier to acquire high quality brainwaves.³³

System-level noise spectrum appears in Figure S5a. Experiments on other noise including motion artifacts appear in Figure S5b and Video S2. Figure 2d-2f shows stable and robust electrical operation of conductive elastomers during several modes of deformations such as twisting (Figure 2d), bending (Figure 2e), and folding (Figure 2f). In all cases, ribbon-shaped nanocomposites (volume, $5 \times 50 \times 0.5 \text{ mm}^3$) were integrated with commercial LEDs to visualize favorable mechanical characteristics. Twisting tests for different angles (red, 0° ; black, 180° ; blue, 360°) indicate negligible variations in fractional changes of impedance, and constant operating features from bending and folding experiments are clearly obvious in the impedance-frequency characteristics. Elastomeric electrodes combined with a soft memory foam enable to reduce elastic modulus. Figure S5c exhibits the stress-strain curve for the comparison of a bulk CNTs-based composite with a soft foam-based system, and calculated young's moduli for each composite are 4 MPa and 40 kPa, respectively. Additional results on mechanical tolerances through a repetitive stretching/fatigue experiment under 30 % of tensile strain appear in Figure S5d. Three-dimensional finite element analysis (3D FEA) reveals the detail mechanics such as strain and pressure distribution associated with wearing process in Figure 2g. (See Figure S6 for additional information). The peak strain and peak interfacial pressure in the ear canal from insertion is 7.6 % and 11 kPa. With an increasing insertion displacement from half to full insertion, the contact area that contributes to the interfacial adhesion increases, leading to an increase in the interfacial pressure averaged over the area of the sensor, while measured electrical properties indicated negligible changes of impedance in response to each pressure during the half to full insertions (Figure 2h). As a result, the best position for EEG monitoring is the full insertion state although the minute changes in contact pressure and impedance occurred.

Figure 3a illustrate an approach to optimize the position of elastomeric conductive electrodes in the ear canal to obtain maximum electric signals from the nervous system via an EEG earphone. Test structures are divided into two modes with respect to the position of a reference electrode: the former placed a reference electrode with upward direction onto the left side of an EEG earphone, while the latter placed it with downward direction onto the same side of an EEG earphone. A ground electrode was placed on the opposite side of a reference electrode. For both cases, source electrodes were positioned onto the right side of an EEG earphone in four different ways, i.e. upward, downward, frontward, and backward. Measured power spectrograms (Figure S4) indicate that alpha rhythms were detected near 10 Hz on every occasion once the test subjects closed their eyes. For the case of attaching a reference electrode on the upward position (Figure 3b), the power amplitude at the upward direction of a source electrode exhibited the highest value than those at any other directions (Figure S7). When a reference electrode was placed on the downward direction, the same tendency in power amplitude was observed although the power spectral density in most cases was much lower than the cases of the upward direction in Figure 3c. The overall results reveal that electrodes position on an EEG earphone plays a critical role of acquiring high quality electrophysiological signals, as which the position of a source and reference electrode becomes closer to the brain, power amplitude approaches the maximum value,³⁴ while the ground electrode needs to be placed a further position from the brain. In addition, wearing the EEG earphone deep inside the ear is beneficial to acquire high quality of brain signal where the sensor becomes closer to the brain.

To demonstrate functionality in useful envisioned areas, we conducted a series of drowsiness detection experiments applicable for efficient learning approach to evaluate or monitor students' ability to concentrate his/her works through a multimedia, and the EEG

earphone could ultimately provide alarms to wake up or refresh. Figure 4a shows an experimental set-up for wireless, real-time monitoring of electrical activities of the brain using an EEG earphone, especially when test subjects were under a drowsy state of consciousness. The operation principle is that test subjects were instructed to push the button to save the response time whenever the logo of 'iBML' changes into the circular red symbol at irregular intervals (Figure 4b). Experimental results shown in Figure 4c to 4e (reaction time, alpha/theta band, and PSD) illustrate related parameters at the wake-sleep transition states, which changes and/or comparison in the recorded EEG data clearly demonstrate that operators were under a sleepy condition. Plots of these saved reaction times given the number of replicates in Figure 4c represent relatively rapid responses in early-stage trials (black dots), however, many errors occurred after approximately 100 trials (red crosses). Here, we defined 'error' as the reaction time that is longer than 700 ms, i.e., test subjects began to fall into a sleepy condition. Such changes in consciousness can be verified with electrophysiological changes using the EEG in a spectrogram analysis of Figure 4d, which exhibited similar tendency of corresponding awaken and drowsy states. For example, alpha wave (8 to 12 Hz) and theta wave (3 to 7 Hz), strongly associated with tired and drowsy states among other waves (e.g. delta and beta waves),³⁵ are slightly oscillated at specific ranges of frequency in awaken state up to 500 seconds, but conversion of conscious state causes oscillation of both waves to increase after 500 seconds compared to those at awaken state. These characteristics are well matched to power spectral density for both states in Figure 4e. Additional relative information about EEG experiments shown in Figure S8.

CONCLUSION

The concept, materials and demonstrations reported here provide a facile approach to produce an earphone to monitor electrophysiological conditions via integration with personal gadgets. Fundamental materials characteristics reveal appropriate electrical and mechanical properties for robust operations, and theoretical considerations support experimental results and future design strategies. Favorable locations of soft electrodes on ear cushions improve the quality of brain signals, and drowsiness studies verify an EEG earphone has capability of detecting sleep onset as well as separation of both sleepy and awoken states. Further researches on a complete integration system of all components including wireless signal acquisition system into the soft electrodes will provide an ultimate form of the EEG earphone.

EXPERIMENTAL SECTION

Fabrication of AgNWs/CNTs/PDMS. To fabricate an elastomeric composite of AgNWs/CNTs/PDMS, each of multiwall CNTs (CM-250, Hanwha Nanotech) and AgNWs (silver nanowires, D: 50 μm , L: 200 μm , ACS Material) were mixed with IPA (2-Propanol, 99.9 %, Sigma-Aldrich) in separate bottles, and the blended solutions were sonicated for 10 minutes to obtain uniform dispersion of materials. A low viscosity silicon oil (PSF-50cSt, Clearco) and PDMS (Sylgard184 A, Dow Corning Corp.) were added into the mixed solution of MWCNTs and AgNWs, then the resulting solution was heated at 60 $^{\circ}\text{C}$ to evaporate the solvent of IPA. Next, addition of a curing agent (Sylgard 184 B, Dow Corning Corp.) and thermal baking procedure at 80 $^{\circ}\text{C}$ for 2 hours formed a flexible, conductive elastomer.

Fabrication of an EEG earphone. A conductive interconnection layer (nickel and copper-based fabric cloth tape, thickness ~ 50 μm) of in-ear cap sensor covered with the gold (thickness ~ 100 nm) and the AgNWs/CNTs/PDMS composite (thickness ~ 200 μm) was attached

to the surface of memory foam substrate. Source, reference, and ground electrodes were defined by similar process. The frame of the EEG earphones was designed and fabricated by the 3D printer (LITHO, Illuminaid). Small speakers were placed inside the earphone frame. The metal layer (copper, thickness $\sim 100\ \mu\text{m}$) was attached to the earphone frame and connected to shielding lines. Every lines were encapsulated by elastic polymer under the thermal contraction tube.

EEG Experiments and Measurements. Ten healthy volunteer subjects with a mean age of 25 ± 3 years were recruited for EEG experiments. Experimental protocol was approved by the Institutional Review Board (IRB No: KU-IRB-15-61-A-1) of Korea University. EEG signals were band-pass filtered ($f_c = 0.5\ \text{Hz}$ to $40\ \text{Hz}$, 3rd order Butterworth), amplified (operational amplifier OP497, gain = 2000), digitized, and sampled with $1\ \text{kHz}$ (AD 974, 16 bit analog to digital converter, Analog Devices Inc.). A microprocessor (ATmega128, Atmel Corp.) wirelessly transmitted EEG signal to personal mobile devices such as a smart phone or a tablet by Bluetooth module (ESD200, SENA). In addition, the acquired signal was analyzed by MATLAB (The Mathworks, Natick, MA, USA, version 2015).

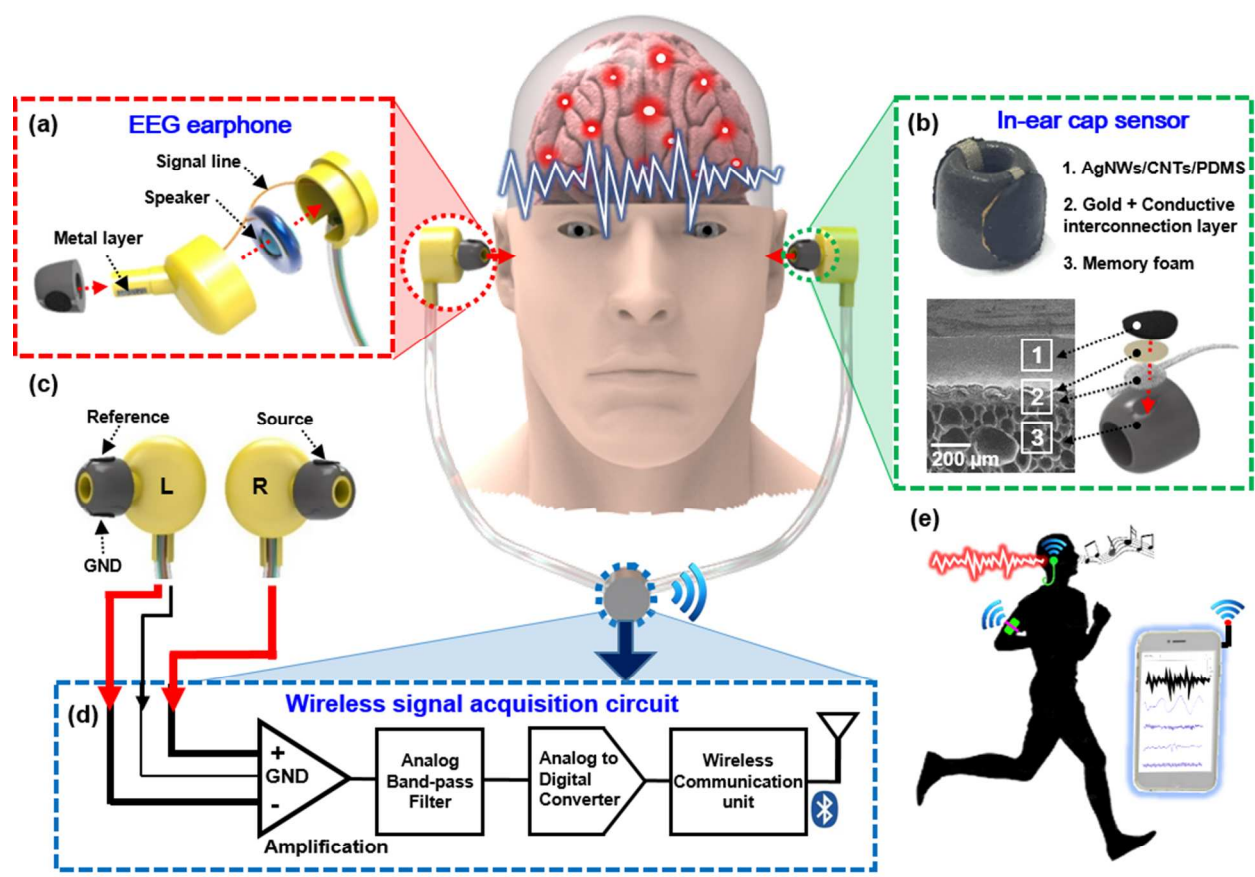


Figure 1. Components and design layout of a personal earphone for recording electrical brain activity. (a) Illustration of structural formation of portable earphones that has capability of real-time measurements of electroencephalogram (EEG). Plastic encasement of earphones includes microphone for sound waves, and electrical signal lines connected to conductive, elastomeric earbuds. (b) Images of detailed structures and elements of fabricated earbud that consists of i) AgNWs/CNTs/PDMS, ii) a conductive interconnection layer covered by a gold layer, and iii) supporting memory foam. (c) Illustration of the placement of each EEG electrodes (source, reference and ground electrodes) that both reference and ground electrodes are located on one side, and the source electrodes on the other side. (d) Schematic description of signal processing block diagram. Obtained real-time brain signals are processed by wireless acquisition circuit which is composed of an amplifier, a bandpass filter, an analog to digital converter, and a

Bluetooth communication unit. (e) The processed EEG data is displayed in real-time on personal devices screen such as a smart phone while in daily life activity.

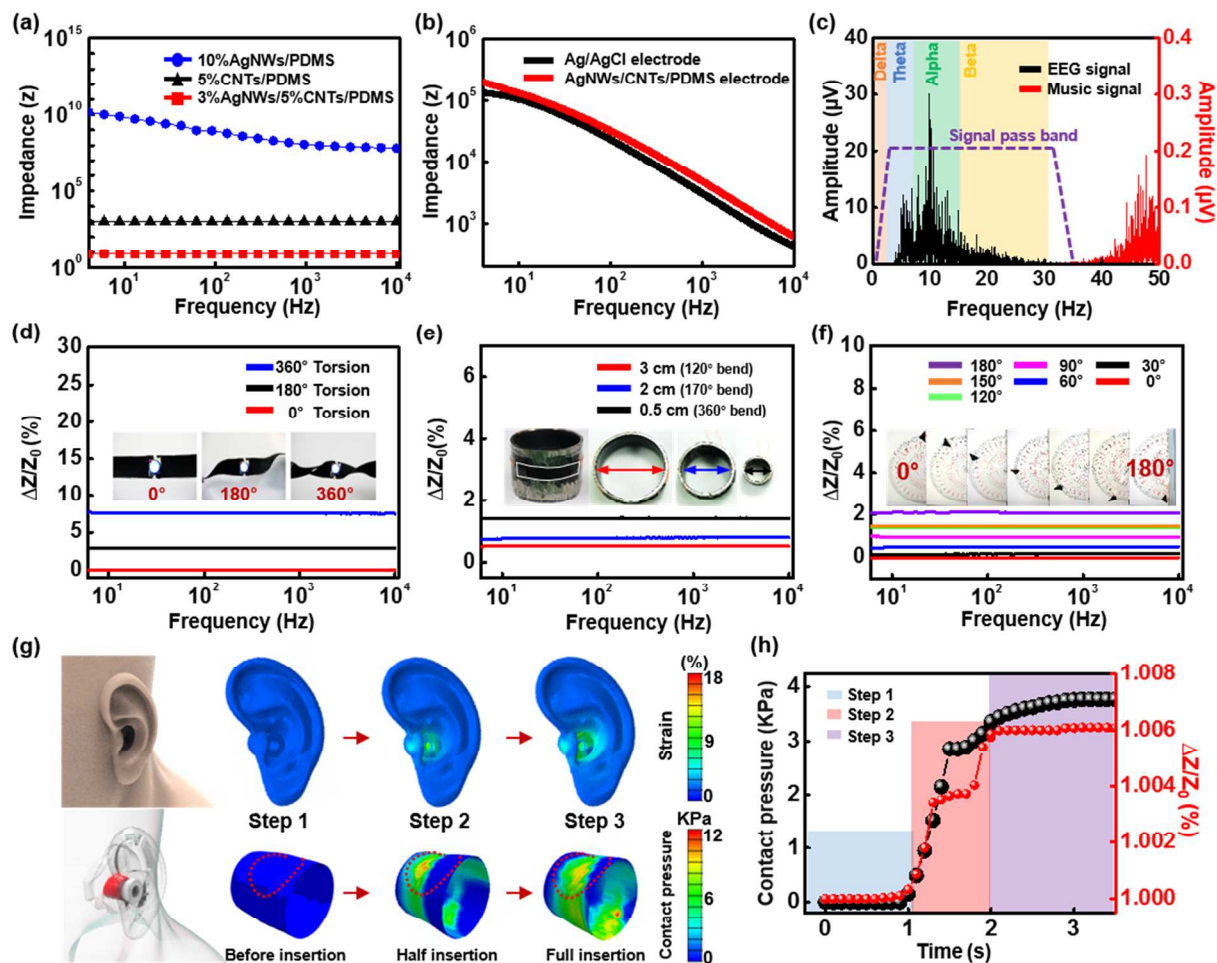


Figure 2. Electrical and mechanical properties of composite materials and sensors. (a) Comparison of measured impedance of composite elastomers, in response to different additives in PDMS (blue, 10 wt % of AgNWs/PDMS; black, 5 wt % of CNTs/PDMS; red, 3 wt % of AgNWs with 5 wt % of CNTs/PDMS). (b) Compared skin and electrode contact impedance electrical property of a commercial, wet electrode of Ag/AgCl with an optimized fabricated, dry electrode of AgNWs/CNTs/PDMS. (c) Simultaneous recording of electrical brain activities and music sounds from a microphone using a representative EEG earphone (black, EEG signal; red, music sound) to demonstrate crosstalk effect. Fractional changes in impedance of conductive composite elastomers at different frequencies during diverse mechanical deformations to verify stability of sensing material, (d) twisting, (e) bending, and (f) folding. (g) Illustration and

1
2
3 calculated distributions of strain and contact pressure while the in-ear cap sensor entering into
4 the ear canal with 3 steps (i.e., before insertion, half insertion, and full insertion). (h) Change of
5 average contact pressure and electrical property on the surface of the sensors (highlighted by red
6 dash lines) from the half (step 2) to full insertion (step 3).
7
8
9
10
11
12
13
14
15
16
17
18
19
20
21
22
23
24
25
26
27
28
29
30
31
32
33
34
35
36
37
38
39
40
41
42
43
44
45
46
47
48
49
50
51
52
53
54
55
56
57
58
59
60

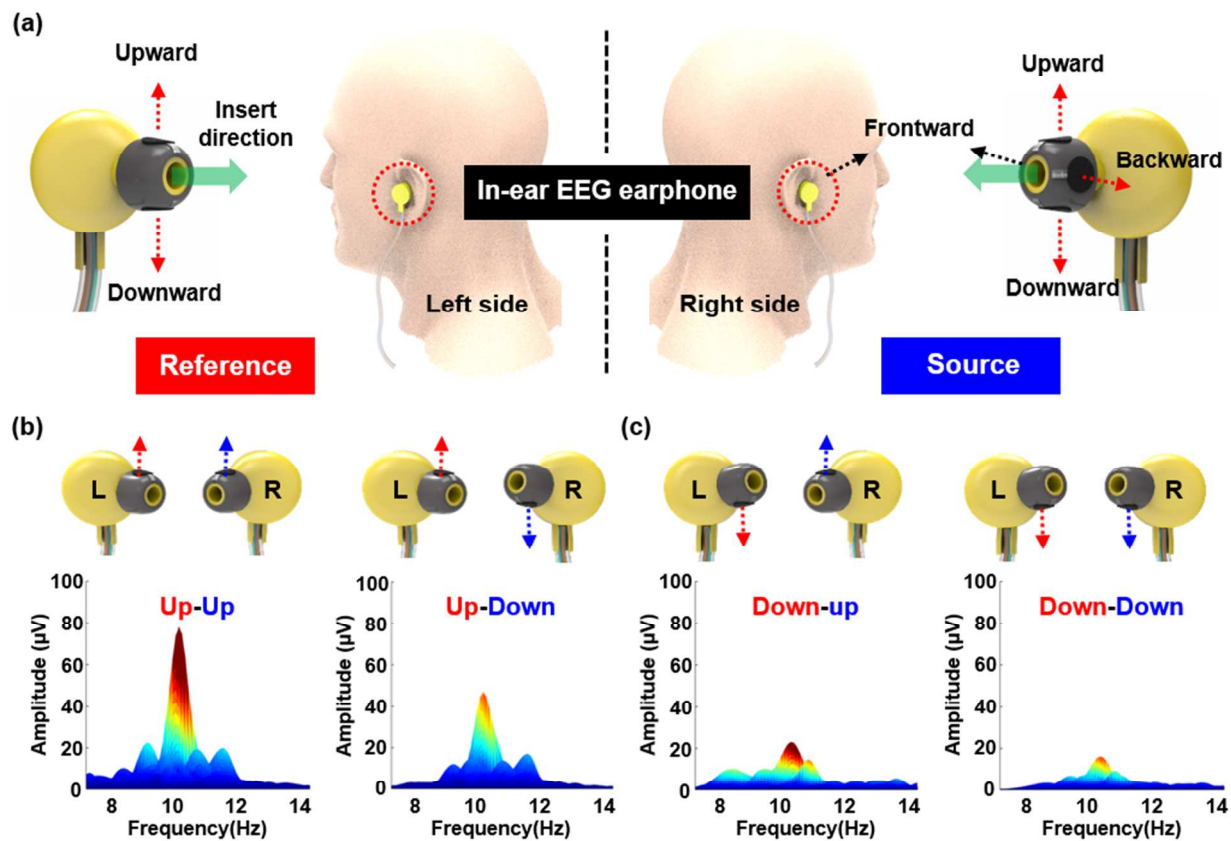


Figure 3. Enhancement of electrical characteristics through optimized placement of electrodes. (a) Description of positioning source, reference and ground electrodes at different sites of memory form-based earbuds. A pair of reference and ground electrodes were placed on the other side of the left earbud, and tested in two different location (upward and downward in related to the position of reference electrodes). Source electrodes on four different locations (upward, downward, frontward, and backward) of the right earbud were tested at the same time for all positions. (b) Experimental results of power spectrogram showing dependence of the recorded EEG amplitudes on relative local positions of electrodes between reference (upward) and source (all directions) electrodes, (c) reference (downward) and source (all directions) electrodes (source electrodes were placed up, down, front and back from left to right frames).

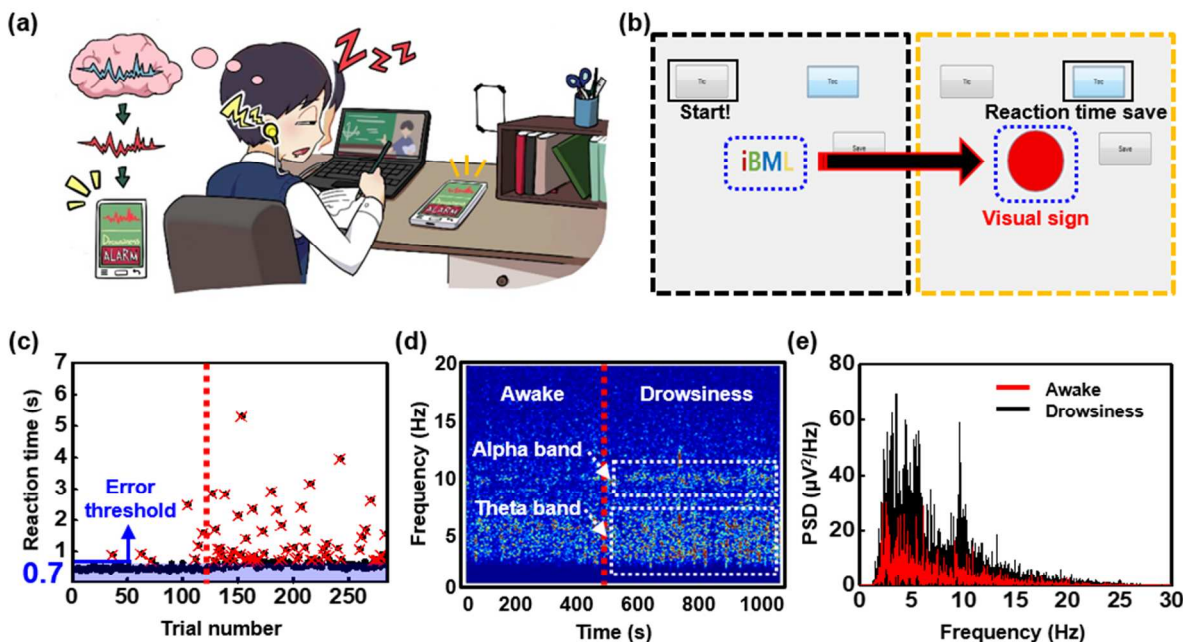


Figure 4. Evaluations of the states of drowsiness as a potential application. (a) Illustration sketch of the wireless in-ear EEG earphone as a way to give alarming through smart phone to person who fall in drowsiness state during working through a multimedia. (b) EEG recording figures with two different control panels on the laptop screen and detailed captured images of control panels consisting of a logo and several buttons for commands and regulations. Test subjects were trained to push the ‘reaction time save’ button to record the response rate when the logo, ‘iBML’ (black box, left), converted into the red circle (yellow box, right) in random timescale. (c) Experimental results of sleep onset over repetitive reactions on transformation of visual signs. Typical errors, i.e. drowsy state, classified when the reaction time is longer than 700 ms (black, each trial; red, classified as errors). (d) Time-frequency analysis of EEG spectrogram representing obvious transitions in both theta and alpha bands, from awake to drowsiness states. (e) Comparison of PSD of EEG signals as analyzed in terms of frequencies while awake (red) and drowsiness conditions (black).

ASSOCIATED CONTENT

Supporting Information

Experimental details of 3D FEA simulations. Schematic of sensor material fabrication (Figure S1); Measurement circuit and systems (Figure S2); SEM images and electrical performances of various conductive materials (Figure S3); EEG recording performance comparing with commercial electrodes (Figure S4); Noise spectrum of system and mechanical performance of sensor (Figure S5); Detailed 3D FEA of sensor strain distribution (Figure S6); Results of detailed sensor position optimization (Figure S7); EEG feasibility results (Figure S8); Introduction of EEG earphone (Video S1); Demonstration of EEG recording in daily life using EEG earphone (Video S2);

AUTHOR INFORMATION

Corresponding Author

*E-mail: dupong76@korea.ac.kr

Notes

The authors declare no competing financial interest.

ACKNOWLEDGMENT

This work was supported by the KU-KIST Graduate School of Converging Science and Technology Program, KU Future Research Grant, and a grant of the Korea Health Technology

R&D Project through the Korea Health Industry Development Institute (KHIDI), funded by the Ministry of Health & Welfare, Republic of Korea (HI14C0771). The authors also acknowledge the Extreme Science and Engineering Discovery Environment (XSEDE) for providing advanced computing resources and services that have contributed to the research results reported in this paper. We note with sadness that Professor S. -H. Lee passed away before submission.

REFERENCES

- (1) Kim, D. -H.; Lu, N.; Ma, R.; Kim, Y. -S.; Kim, R. -H.; Wang, S.; Wu, J.; Won, S. M.; Tao, H.; Islam, A.; Yu, K. J.; Kim, T. I.; Chowdhury, R.; Ying, M.; Xu, L.; Li, M.; Chung, H. -J.; Keum, H.; McCormick, M.; Liu, P.; Zhang, Y. -W.; Omenetto, F. G.; Huang, Y.; Coleman, T.; Rogers, J. A. Epidermal electronics. *Science* **2011**, *333*, 838-843.
- (2) Jeong, J. -W.; Yeo, W. -H.; Akhtar, A.; Norton, J. J.; Kwack, Y. -J.; Li, S.; Jung, S. -Y.; Su, Y.; Lee, W.; Xia, J.; Cheng, H.; Huang, Y.; Choi, W. -S.; Bretl, T.; Rogers, J. A. Materials and optimized designs for human-machine interfaces via epidermal electronics. *Adv. Mater.* **2013**, *25*, 6839-6846.
- (3) Yeo, W. -H.; Kim, Y. -S.; Lee, J.; Ameen, A.; Shi, L.; Li, M.; Wang, S.; Ma, R.; Jin, S. H.; Kang, Z.; Huang, Y.; Rogers, J. A. Multifunctional epidermal electronics printed directly onto the skin. *Adv. Mater.* **2013**, *25*, 2773-2778.
- (4) Someya, T.; Sekitani, T.; Iba, S.; Kato, Y.; Kawaguchi, H.; Sakurai, T. A large-area, flexible pressure sensor matrix with organic field-effect transistors for artificial skin applications. *P. Natl. Acad. Sci. USA* **2004**, *101*, 9966-9970.

(5) Park, J.; Choi, S.; Janardhan, A. H.; Lee, S. -Y.; Raut, S.; Soares, J.; Shin, K.; Yang, S. X.; Lee, C.; Kang, K. -W.; Cho, H. R.; Kim, S. J.; Seo, P.; Hyun, W.; Jung, S.; Lee, H. -J.; Lee, N.; Choi, S. H.; Sacks, M.; Lu, N. S.; Josephson, M. E.; Hyeon, T.; Kim, D. -H.; Hwang, H. J. Electromechanical cardioplasty using a wrapped elasto-conductive epicardial mesh. *Sci. Transl. Med.* **2016**, *8*, 344ra86.

(6) Viventi, J.; Kim, D. -H.; Vigeland, L.; Frechette, E. S.; Blanco, J. A.; Kim, Y. -S.; Avrin, A. E.; Tiruvadi, V. R.; Hwang, S. -W.; Vanleer, A. C.; Wulsin, D. F.; Davis, K.; Gelber, C. E.; Palmer, L.; Van der Spiegel, J.; Wu, J.; Xiao, J. L.; Huang, Y. G.; Contreras, D.; Rogers, J. A.; Litt, B. Flexible, foldable, actively multiplexed, high-density electrode array for mapping brain activity in vivo. *Nat. Neurosci.* **2011**, *14*, 1599-1605.

(7) Xu, L.; Gutbrod, S. R.; Bonifas, A. P.; Su, Y.; Sulkin, M. S.; Lu, N.; Chung, H. -J.; Jang, K. -I.; Liu, Z.; Ying, M.; Lu, C.; Webb, R. C.; Kim, J. -S.; Laughner, J. I.; Cheng, H.; Liu, Y.; Ameen, A.; Jeong, J. -W.; Kim, G. -T.; Huang, Y.; Efimov, I. R.; Rogers, J. A. 3D multifunctional integumentary membranes for spatiotemporal cardiac measurements and stimulation across the entire epicardium. *Nat. Commun.* **2014**, *5*, 3329.

(8) Khodagholy, D.; Gelinas, J. N.; Thesen, T.; Doyle, W.; Devinsky, O.; Malliaras, G. G.; Buzsaki, G. NeuroGrid: recording action potentials from the surface of the brain. *Nat. Neurosci.* **2015**, *18*, 310-315.

(9) Jang, K. -I.; Chung, H. U.; Xu, S.; Lee, C. H.; Luan, H. W.; Jeong, J.; Cheng, H. Y.; Kim, G. -T.; Han, S. Y.; Lee, J. W.; Kim, J.; Cho, M.; Miao, F. X.; Yang, Y. Y.; Jung, H. N.; Flavin, M.; Liu, H.; Kong, G. W.; Yu, K. J.; Rhee, S. I.; Chung, J.; Kim, B.; Kwak, J. W.; Yun, M. H.;

Kim, J. Y.; Song, Y. M.; Paik, U.; Zhang, Y. H.; Huang, Y.; Rogers, J. A. Soft network composite materials with deterministic and bio-inspired designs. *Nat. Commun.* **2015**, *6*, 6566.

(10) Kaltenbrunner, M.; Sekitani, T.; Reeder, J.; Yokota, T.; Kuribara, K.; Tokuhara, T.; Drack, M.; Schwodiauer, R.; Graz, I.; Bauer-Gogonea, S.; Bauer, S.; Someya, T. An ultra-lightweight design for imperceptible plastic electronics. *Nature* **2013**, *499*, 458.

(11) Fan, J. A.; Yeo, W. -H.; Su, Y. W.; Hattori, Y.; Lee, W.; Jung, S. -Y.; Zhang, Y. H.; Liu, Z. J.; Cheng, H. Y.; Falgout, L.; Bajema, M.; Coleman, T.; Gregoire, D.; Larsen, R. J.; Huang, Y. G.; Rogers, J. A. Fractal design concepts for stretchable electronics. *Nat. Commun.* **2014**, *5*, 3266.

(12) Shin, M.; Song, J. H.; Lim, G. -H.; Lim, B.; Park, J. -J.; Jeong, U. Highly Stretchable Polymer Transistors Consisting Entirely of Stretchable Device Components. *Adv. Mater.* **2014**, *26*, 3706-3711.

(13) Oh, J. Y.; Kim, S.; Baik, H. -K.; Jeong, U. Conducting Polymer Dough for Deformable Electronics. *Adv. Mater.* **2016**, *28*, 4455-4461.

(14) Wang, Y.; Zhu, C.; Pfattner, R.; Yan, H.; Jin, L.; Chen, S.; Molina-Lopez, F.; Lissel, F.; Liu, J.; Rabiah, N. I.; Chen, Z.; Chung, J. W.; Linder, C.; Toney, M. F.; Murmann, B.; Bao, Z. A highly stretchable, transparent, and conductive polymer. *Sci. Adv.* **2017**, *3*, e1602076.

(15) Gong, S.; Schwalb, W.; Wang, Y. W.; Chen, Y.; Tang, Y.; Si, J.; Shirinzadeh, B.; Cheng, W. L. A wearable and highly sensitive pressure sensor with ultrathin gold nanowires. *Nat. Commun.* **2014**, *5*, 3132.

(16) Yao, S.; Zhu, Y. Wearable multifunctional sensors using printed stretchable conductors made of silver nanowires. *Nanoscale* **2014**, *6*, 2345-2352.

(17) Takei, K.; Yu, Z.; Zheng, M.; Ota, H.; Takahashi, T.; Javey, A. Highly sensitive electronic whiskers based on patterned carbon nanotube and silver nanoparticle composite films. *Proc. Natl. Acad. Sci. U S A* **2014**, *111*, 1703-1707.

(18) Chen, Z.; To, J. W. F.; Wang, C.; Lu, Z. D.; Liu, N.; Chortos, A.; Pan, L. J.; Wei, F.; Cui, Y.; Bao, Z. A Three-Dimensionally Interconnected Carbon Nanotube-Conducting Polymer Hydrogel Network for High-Performance Flexible Battery Electrodes. *Adv. Energy Mater.* **2014**, *4*, 1400207.

(19) Lipomi, D. J.; Vosgueritchian, M.; Tee, B. C.; Hellstrom, S. L.; Lee, J. A.; Fox, C. H.; Bao, Z. Skin-like pressure and strain sensors based on transparent elastic films of carbon nanotubes. *Nat. Nanotechnol.* **2011**, *6*, 788-792.

(20) Chen, K.; Gao, W.; Emaminejad, S.; Kiriya, D.; Ota, H.; Nyein, H. Y.; Takei, K.; Javey, A. Carbon Nanotubes: Printed Carbon Nanotube Electronics and Sensor Systems (Adv. Mater. *22/2016*). *Adv. Mater.* **2016**, *28*, 4397-4414.

(21) Lee, S.; Reuveny, A.; Reeder, J.; Lee, S.; Jin, H.; Liu, Q.; Yokota, T.; Sekitani, T.; Isoyama, T.; Abe, Y.; Suo, Z.; Someya, T. A transparent bending-insensitive pressure sensor. *Nat. Nanotechnol.* **2016**, *11*, 472-478.

(22) Sekitani, T.; Nakajima, H.; Maeda, H.; Fukushima, T.; Aida, T.; Hata, K.; Someya, T. Stretchable active-matrix organic light-emitting diode display using printable elastic conductors. *Nat. Mater.* **2009**, *8*, 494-499.

(23) Yun, Y. J.; Ju, J.; Lee, J. H.; Moon, S. -H.; Park, S. -J.; Kim, Y. H.; Hong, W. G.; Ha, D. H.; Jang, H.; Lee, G. H.; Chung, H. -M.; Choi, J.; Nam, S. W.; Lee, S. -H.; Jun, Y. Highly Elastic Graphene-Based Electronics Toward Electronic Skin. *Adv. Funct. Mater.* **2017**, *27*, 1701513.

(24) Ameri, S. K.; Ho, R.; Jang, H. W.; Tao, L.; Wang, Y. H.; Wang, L.; Schnyer, D. M.; Akinwande, D.; Lu, N. S. Graphene Electronic Tattoo Sensors. *Acs Nano* **2017**, *11*, 7634-7641.

(25) Liu, N.; Chortos, A.; Lei, T.; Jin, L.; Kim, T. R.; Bae, W. -G.; Zhu, C.; Wang, S.; Pfattner, R.; Chen, X.; Sinclair, R.; Bao, Z. Ultratransparent and stretchable graphene electrodes. *Sci. Adv.* **2017**, *3*, e1700159.

(26) Ding, Y.; Xu, W.; Wang, W.; Fong, H.; Zhu, Z. Scalable and Facile Preparation of Highly Stretchable Electrospun PEDOT:PSS@PU Fibrous Nonwovens toward Wearable Conductive Textile Applications. *ACS Appl. Mater. Interfaces* **2017**, *9*, 30014-30023.

(27) Yao, S.; Swetha, P.; Zhu, Y. Nanomaterial-Enabled Wearable Sensors for Healthcare. *Adv. Health. Mater.* **2017**, *7*, 1700889.

(28) Yao, S.; Zhu, Y. Nanomaterial-enabled stretchable conductors: strategies, materials and devices. *Adv. Mater.* **2015**, *27*, 1480-1511.

(29) Myers, A. C.; Huang, H.; Zhu, Y. Wearable silver nanowire dry electrodes for electrophysiological sensing. *RSC Adv.* **2015**, *5(15)*, 11627-11632.

(30) Lee, J. H.; Lee, S. M.; Byeon, H. J.; Hong, J. S.; Park, K. S.; Lee, S. -H. CNT/PDMS-based canal-typed ear electrodes for inconspicuous EEG recording. *J. Neural. Eng.* **2014**, *11*, 046014.

1
2
3
4
5
6
7
8
9
10
11
12
13
14
15
16
17
18
19
20
21
22
23
24
25
26
27
28
29
30
31
32
33
34
35
36
37
38
39
40
41
42
43
44
45
46
47
48
49
50
51
52
53
54
55
56
57
58
59
60

(31) Rosen, S.; Howell, P. Signals and systems for speech and hearing. *Brill* **2011**, 29, 163-164.

(32) Teplan, M. Fundamentals of EEG measurement. *Measurement science review* **2002**, 2, 1-11.

(33) Wilson, J. A.; Guger, C.; Schalk, G. BCI hardware and software. *Brain-computer interfaces: principles and practice* **2012**, 165-188.

(34) Debener, S.; Emkes, R.; De Vos, M.; Bleichner, M. Unobtrusive ambulatory EEG using a smartphone and flexible printed electrodes around the ear. *Sci. Rep-Uk* **2015**, 5, 16743.

(35) Craig, A.; Tran, Y.; Wijesuriya, N.; Nguyen, H. Regional brain wave activity changes associated with fatigue. *Psychophysiology* **2012**, 49, 574-582.

Table of contents figure

